International Journal of Electrical, Electronic and Communication Sciences
ISSN: 2517-9438
Vol:5, No:8, 2011

Effect of Uneven Surface on Magnetic Properties of Fe-Based Amorphous Transformer

Yeong-Hwa Chang, Chang-Hung Hsu, Huei-Lung Chu, Chia-Wen Chang, Wei-Shou Chan, Chun-Yao Lee; Chia-Shiang Yao and Yan-Lou He

***Abstract*—**This study reports the preparation of soft magnetic ribbons of Fe-based amorphous alloys using the single-roller melt-spinning technique. Ribbon width varied from 142 mm to 213 mm and, with a thickness of approximately 22 μm ± 2 μm. The microstructure and magnetic properties of the ribbons were characterized by differential scanning calorimeter (DSC), X-ray diffraction (XRD), vibrating sample magnetometer (VSM), and electrical resistivity measurements (ERM). The amorphous material properties dependence of the cooling rate and nozzle pressure have uneven surface in ribbon thicknesses are investigated. Magnetic measurement results indicate that some region of the ribbon exhibits good magnetic properties, higher saturation induction and lower coercivity. However, due to the uneven surface of 213 mm wide ribbon, the magnetic responses are not uniformly distributed. To understand the transformer magnetic performances, this study analyzes the measurements of a three-phase 2 MVA amorphous-cored transformer. Experimental results confirm that the transformer with a ribbon width of 142 mm has better magnetic properties in terms of lower core loss, exciting power, and audible noise.

***Keywords*—**Amorphous ribbon, uneven surface, magnetic properties, and rapid solidification

I. Introduction

FE-BASED amorphous ribbons are often used as soft magnetic materials because of their high permeability and low coercivity [1-4]. However, these alloys become brittle upon annealing, which causes serious difficulties in handling process and material volume in different thickness. Previous studies [5, 6] investigate the coercivity, remanence, and permeability of Fe-based amorphous ribbons of various magnetisms in rapidly quenched rate processes. This suggests that the controlled partial crystallization of this alloy can lead to the formation of crystalline phase with excellent soft magnetic properties. One study [7] investigates the correlation between observed changes in the magnetic properties and different aspects of quenched rate in material thickness. Quenched-in internal stresses significantly influence the soft magnetic properties.For different annealing procedures of amorphous materials [8-11], the variations of magnetic properties of Fe-based amorphous cores were investigated. The giant magnetoimpedance of Fe-based nanocomposite materials in microstructures and the magnetic properties were significantly affected by the different annealing processes. Heat treatments of the ribbon below the first crystallization temperature yielded a soft magnetic phase of a-Fe (Si) embedded in the amorphous phase [12]. It was also discovered that the crystallization phenomenon of a-Fe (Si) under different annealing temperatures will be changed in magnetic properties, which including coercivity, remanence and saturation magnetization can be obtained. Moreover, the electrical resistivity of physical characteristics of Fe-based amorphous ribbons was measured at room temperatures [13]. According to the measured results, the electrical resistivities of amorphous ribbons were varied under different annealing temperatures. Besides, electrical and dielectric properties for regulated material composition by doping chromium into Fe-based amorphous alloys can be obtained [14]. In [15], the crystallization process and the effect of copper addition on magnetic properties of Fe-based amorphous alloys were investigated by using differential scanning calorimeter (DSC) and X-ray diffraction meter (XRD). For different annealing temperature addition material composition, it was discovered that the main reasons causing the variation of magnetic properties of amorphous alloys are investigated. So, amorphous material in magnetic properties such as saturation magnetic induction, coercivity, remanence, permeability and resistivity were considered as the dominant factors having affection on material magnetization. Previous research shows that the quenching rate of a ribbon directly influences its magnetic properties. However, the two surfaces of Fe-Nb-B ribbons exhibit different properties [16-18]. It is concentrated that the material crystallization in a very thin layer at the surface is typical for the wheel side. The parameters of the coercive fields are different for the wheel and shiny sides. However, existing studies do not explore the effects of an uneven surface on the magnetic properties of different ribbon widths for Fe-based amorphous-cored SA1 transformer applications. However, the magnetic properties related to different ribbon widths are still far from a complete understanding. Except for the aforementioned annealing procedure and composition regulated in materials, the process of ribbon manufacturing is also an important factor to affect the magnetic properties. This study systematically explores the dependence of hysteresis loop parameters and the orientation of local magnetization on a ribbon measuring 22 μm ± 2 μm thick. The ribbon specification in different width of 142 mm to 213 mm of amorphous materials

Corresponding author: Dr. C.-H. Hsu is with the Fortune Electrical Company Ltd. He is currently project manager (phone: +886-3-4526111 (e-mail: chshiu@fortune.com.tw).

Dr. Y.-H Chang is with the Chang Gung University, Department of Electrical Engineering, He is currently an associate professor.

Mr. Huei-Lung Chu, Chia-Shiang Yao, and Yan-Lou He are with Fortune Electric Company Ltd and Chung Yuan Christian University.

Dr. Chia-Wen Chang, and Wei-Shou Chan are with Chang Gung University.

Dr. Chun-Yao Lee is with Chung Yuan Christian University; he is currently an assistant professor.

is used. Section II describes the experimental procedure. Section III uses DSC, XRD, VSM, and ERM to analyze the magnetic properties of the ribbon at various thicknesses. Section IV analyzes the magnetic properties of three-phase transformer. Finally, Section V offers a summary and conclusion.

II. Experimentation Method

Fe-based amorphous alloy SA1 was fabricated by melting the appropriate proportions of iron, silicon, and boron elements in an argon atmosphere. Figure 1 shows how rapidly solidified ribbons were manufactured by the single-roller melt-spinning technique. Using this technique, it is possible to quench the molten alloy at a cooling rate of approximately 10^4-10^6 K/s. This study analyzes the alloy surface controlling the iron source-containing amount of the amorphous alloy ribbon composition, and controlling gas atmosphere around the cooling roller of the nozzle tip part in the case of the ribbon.

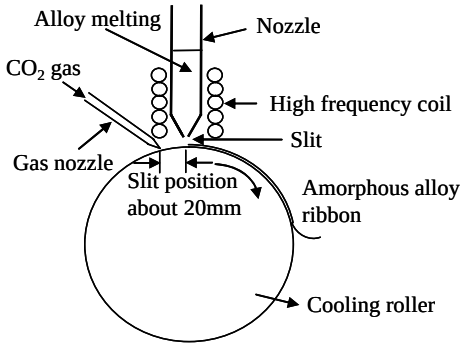

Fig. 1 Scheme diagram of single-roller rapid solidification technique

In Figure 2, it is illustrates that the resulting samples had different widths from regions A to D. In Figure 3, it shows the measured results for samples with different thicknesses, indicating that the ribbon thickness is approximately 22 μm ± 2 μm. To determine the magnetic properties of samples, the amorphous/crystalline nature of the samples after annealing is characterized using the X-ray diffractometry (XRD) technique. The XRD experiments are performed using a Bruker (D8SSS) with filtered CuKα (λ=0.154056 nm), 40 kV and 40 mA. The differential scanning calorimetry (DSC) (SDT 2960) showed the crystallization of rapidly solidified ribbons for both continuous heating and isothermal annealing in a pure argon atmosphere. The magnetic measurements of the vibrating sample magnetometers (LakeShore 7404) are used to characterize the DC magnetic properties of the material as a function of magnetic field, temperature, and time. Then, the electrical resistivities of the samples are measured using the four-probe method.

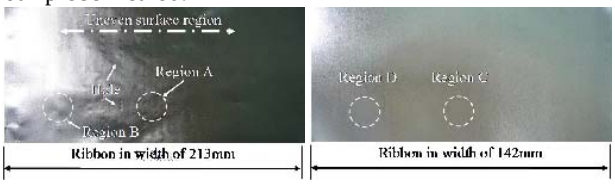

(a) (b)

Fig. 2 Photographs of amorphous alloy ribbons in different widths: (a) 213 mm, (b) 142 mm

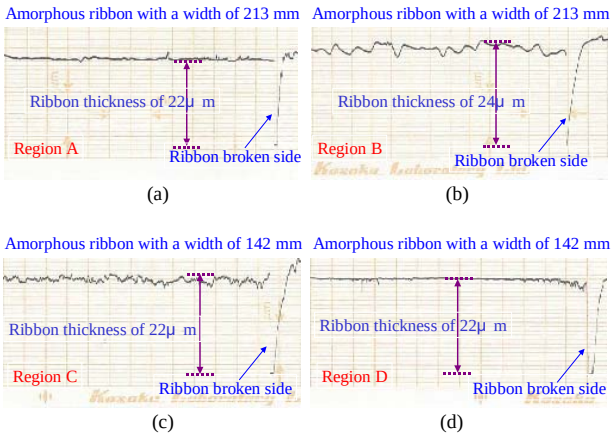

Fig. 3 The thicknesses of amorphous ribbons: samples taken from (a) and (b) in widths of 213 mm, and samples taken from (c) and (d) in widths of 142 mm.

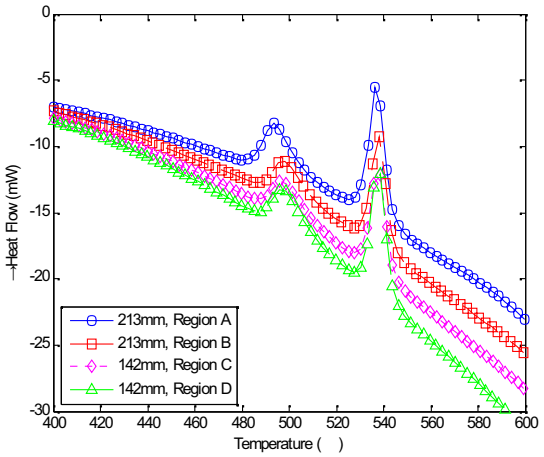

Fig. 4 DSC curves of different ribbon samples.

III. Magnetization Analysis and Measurement

A. DSC

The DSC curves in Fig. 4 show two exothermic events corresponding to the crystallization process. The material crystalline temperature for the ribbon of 213 mm width is different as that of the ribbon with a width of 142 mm. This indicates that the exothermic peaks were taken from different samples. Table 1 summarizes the parameters of crystalline reaction. The volume fraction of crystalline phase is roughly approximately 1.34% indicating that the volume fraction probably induced a good magnetic property in the ribbon with a width of 213 mm in region A. From Fig. 4, it can be seen that the exothermic peaks occur when the annealing temperature exceeds 493 °C. In such circumstances, the amorphous samples

become fully crystallized [17]. Note that the behavior of excessive crystallization may degrade the magnetic properties of soft ribbons. The reason is that annealing temperature exceeding the crystalline temperature will induce the growing of the body centered cubic (BCC) structure of α-Fe crystallites. Because the magnetocrystalline anisotropy is the energy cost per atom to align its magnetization from one crystallographic direction to another. In other words, large crystallites will lead magnetic properties changing from ferromagnetic to paramagnetic, that could result in the degrade of magnetic properties.

TABLE I
THE EXOTHERMIC PEAK VALUES FROM THE DSC CURVES

Specification	Region A	Region B	Region C	Region D
Primary peak	493.38	497.4	497	496.94
Secondary peak	537.04	537.85	537.74	537.74

B. XRD

The XRD measurements in Fig. 5 reveal the crystallization properties of amorphous ribbons. According to the Bragg's law, it can be observed that the diffraction 2θ around 44.5° has higher crystalline peak of α-Fe. The ferromagnetism of the amorphous phase gradually translated to paramagnetic behavior as the crystalline grain affected the magnetic properties of the amorphous materials. Equation (1) shows Scherrer's formula

$$d = \frac{k\lambda}{\beta \cos\theta} \quad (1)$$

where d is the grain size (diameter), k is a constant value 0.9, λ is the X-ray wave length (λ=0.15405 nm), β is the breadth (full-width at half-maximum) of the peak, and θ is the diffraction peak angle. After annealing all samples, the thickness of the ribbons is approximately 22 μm ± 2 μm and ribbon widths are 213 mm and 142 mm, respectively. This paper shows that the values of full-width at half-maximum of the broad diffraction peak located at 2θ are approximately 44.4° in the XRD patterns. These results suggest the α-Fe in bcc-iron (110). Fig. 6shows the different material samples and average grain sizes in crystalline α-Fe The amorphous alloy in widths of 213 mm can be easily broken because it has significant uneven surface than others. Results show that the grain size of region A has smaller crystalline α-Fe particles with higher magnetic properties than that sample of region B.

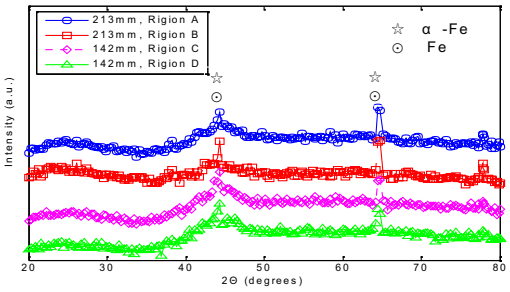

Fig. 5 XRD measured results of different ribbon samples

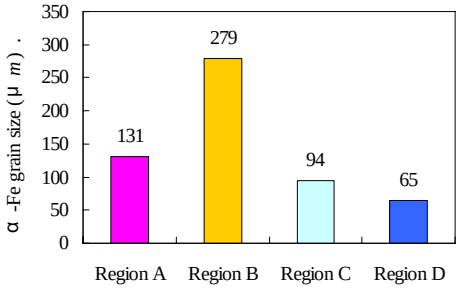

Fig. 6 The grain sizes of the α-Fe for amorphous ribbons, annealing at 350 °C, 2h

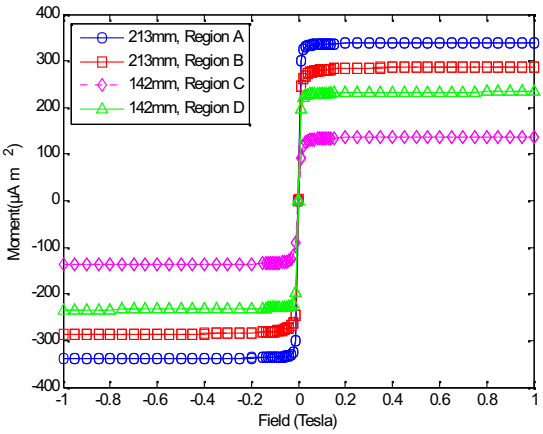

Fig. 7 The measured results of magnetic properties identified by VSM

TABLE II
MAGNETIC PARAMETERS OF FE-BASED AMORPHOUS RIBBON ANNEALED AT 350°C, 2H

Measured Parameter	$M_s \times 10^{-3}$ (μA/m^{-2})	$M_r \times 10^{-7}$ (μA/m^{-2})	Hc $\times 10^{-5}$ (Tesla)	M_s/M_r $\times 10^{-4}$	ρ (mΩ-cm)
Region A	0.339065	3.965	1.316	1.169	0.572
Region B	0.287065	13.4	5.432	4.681	0.311
Region C	0.13759	1.698	1.855	1.234	0.478
Region D	0.2339	4.015	2.034	1.717	0.492

C. VSM

Figure 7 measures the hysteresis loop of the amorphous ribbon at room temperature. Magnetic parameters such as saturation magnetization (M_s), remanent magnetization (M_r), and coercivity (Hc) can be identified by VSM. Table II lists the results of magnetism parameter measurements. This table shows that the case of 213 mm has higher M_s and lower Hc because the crystalline grain size of α-Fe is significantly larger than 142 mm.Besides, for squareness ratio parameter [10], the M_r/M_s ratio of the proposed sample for the width of 213 mm in region A sample is smaller than that in region B. For region C and D, with the grain size of α-Fe particles, it is necessary to increase coercivity due to the uneven surface and thickness of samples.

D. ERM

The electrical resistivity ρ is measured at room temperature. The parameter of the electrical resistivity was measured by ERM after the annealing process. DSC and XRD analysis confirmed the variation of electrical resistivity for different ribbon widths. Table II lists the electrical resistivities for both ribbon samples in different widths. Results show that the electrical resistivity of the 142 mm ribbon was smoother than the 213 mm ribbon. Therefore, the eddy losses of amorphous ribbon with measuring 142mm wide are significantly reduced.

IV. Magnetic Properties of Three-Phase Amorphous-Cored Transformer

The experiments in this study used Fe-based amorphous alloys to implement transformer cores with 142mm and 213mm ribbons. To achieve low core loss, the annealing temperature is set at 350°C and allowed to proceed for 2h in an nitrogen atmosphere with an applied 800 A/m dc magnetic field. Figure 8 shows the three-phase power transformer fabricated and tested. Test results indicate the core loss and exciting power of the Fe-based amorphous-cored transformer with the 142 mm ribbon were relatively lower, as Fig. 9(a) and 9(b) illustrate. The core loss of the 142mm ribbon was less than that of the 213 mm ribbon. The required exciting power of the 142 mm ribbon was slightly less than that of the 213mm ribbon. The exciting power increased when the magnetic induction was larger than 1.3 (T). In Fig. 9(c), it shows the measurements of audible noise with respect to different width ribbons. In summary, the audible noise of the 213mm ribbon was greater than that of the 142mm ribbon.

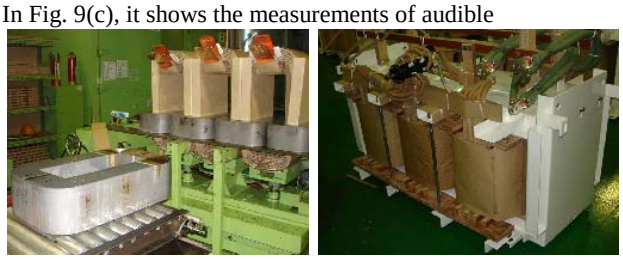

(a) (b)

Fig. 8 Arrangement and fabrication of an amorphous transformer with capacity 2MVA: (a) core and winding assembling, (b) construction of 2MVA three-phase transformer

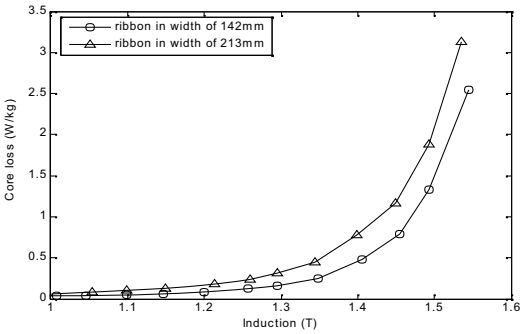

(a)

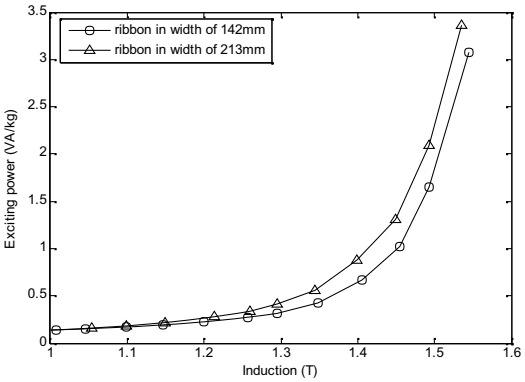

(b)

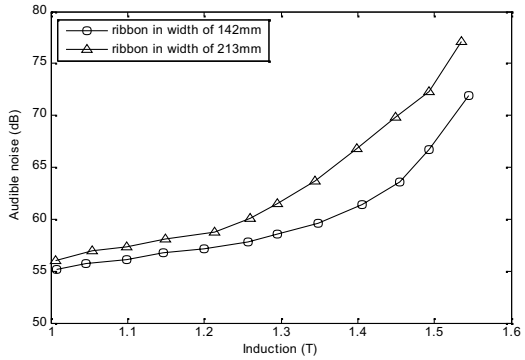

(c)

Fig. 9 Measured results of 3-phase 2MVA amorphous-cored transformers: (a) core loss, (b) exciting power, (c) audible noise

V. Conclusion

This study investigates the magnetic properties and crystalline structures of Fe-based amorphous alloys with various ribbon thicknesses (22 μm ± 2 μm). DSC analysis shows that the exothermic heat of crystallization for the ribbon width of 213 mm in middle part is approximately 1.32%. According to XRD results, the middle part of the 213 mm ribbon has smaller α-Fe particles, while VSM results indicate higher magnetic

induction and lower coercivity. However, a uniform magnetic property of 213 mm wide ribbon is not available due to the uneven surface of amorphous ribbon. That will also affect the associated magnetic properties of amorphous-cored transformers. Finally, a three-phase amorphous-cored transformer with different ribbon widths was fabricated. Results show that the ribbon measuring 142mm wide exhibited better magnetic properties in terms of lower core loss, exciting power, and audible noise.

REFERENCES

[1] D. Azuma and R. Hasegawa, "Audible noise from amorphous metal and silicon steel-based transformer core," *IEEE Trans. Magn.*, vol. 44, no. 11, pp. 4104-4106, Nov., 2008.

[2] E. N. Andreev, L. I. Chubraeva, "Investigation of a model HTSC transformer with amorphous alloy cores," *J. Mate. Pro. Tech.*, vol. 181, no. 1-3, pp. 25-30, Jan., 2007.

[3] Y. Ogawa, M. Naoe, Y. Yoshizawa, et. al., "Magnetic properties of high Bs Fe-based amorphous material,"*J. Magn. Magn. Mate.*, vol. 304, no. 2, pp. e675-e677, Sep., 2006.

[4] R. Hasegawa, "Applications of amorphous magnetic alloys," *Mate. Sci. Eng. A*, vol. 375-377, no. 15, pp. 90-97, Jul. 2004.

[5] N. Mattern, "Structure formation in liquid and amorphous metallic alloys," *J. Non-Cry. Sol.*, vol. 353, no. 18-21, pp. 1723-1731, Jun., 2007.

[6] M. García del Muro, R. Zquiak, and X. Batlle, "The effect of quenching rate on the nanocrystallization of amorphous FeCuNbSiB,"*J Magn. Magn. Mate.*,vol. 171, no. 3, pp. 315-319, Jul., 1997.

[7] A. K. Panda, S. Roy, S. R. Singh, et. al., "Effect of quenching rate on the properties of melt-spun FeNbCuSIB ribbons,"*J. Mate. Sci. Eng. A,* vol. 304-306, no. 31, pp. 457-461, May, 2001.

[8] W. S. D. Folly, V. R. Caffarena, R. L. Sommer, J. L. Capitaneo, and A. P. Guimarães, "Magnetic properties of $Fe_{90}Zr_7B_3$ ribbons studied by FMR and magnetization, "*J. Magn. Magn. Mater*, vol. 320, no. 14, pp. e358-e361, July. 2008.

[9] Y. C. Niu, X. F. Bian, W. M. Wang, G .H. Li, S. F. Jin, and Q. Jia, " On the distinct tensile flow of amorphous $Fe_{78}Si_9B_{13}$ alloy at 430 ℃ during continuous annealing, " *J. Alloys and Comp*., vol. 462, no. 1-2, pp. 362-366, Aug. 2008.

[10] D.M. Minić, A. Maričić, and B. Adnađević, "Crystallization of α-Fe phase in amorphous $Fe_{81}B_{13}Si_4C_2$ alloy, "*J. Alloys and Comp*. vol. 473, no. 1-2, pp. 363-367, Apr., 2009.

[11] M. H. Phan, H. X. Peng, M. R. Wisnom, S. C. and N. Chau, "Effect of annealing on the microstructure and magnetic properties of Fe-based nanocomposite materials, "*Appl. Sci. Manu. Comp. Part A*, vol. 37, no, 2, pp, 191-196, Feb., 2006.

[12] W. Pon-On, P. Winotai, and I. M. Tang, "Nanocrystallization in $Fe_{81}B_{13.5}Si_{3.5}C_2$ amorphous magnetic ribbons, "*J. Magn. Magn. Mater*,. vol. 320, no. 3-4, pp. 81-91, Feb., 2008.

[13] W. M. Wanga, Y. C. Niua, F. Wangb, J. C. Lianga, S. F. Jina, W. G. Zhanga and X.F. Biana, "Electrical resistivity evolution in the annealed amorphous $Fe_{78}Si_9B_{13}$ ribbons, " *J. Non-Crys. Sol.*, vol. 354, no, 30, pp. 3612-3616, Jul. 2008.

[14] J. I. Muhammad and A. K. Rafaqat, "Enhancement of electrical and dielectric properties of Cr doped $BaZn_2$ W-type hexaferrite for potential applications in high frequency devices, " *J. Alloys and Comp.*, vol. 478, no. 1-2, pp. 847-852, Jun. 2009.

[15] H. T. Zhou, Z. K. Zhao, X. Zhou, B. Yan, J. W. Zhong, and Q. B. Li, "The peculiarities of the nanocrystallization process and copper addition effects for an amorphous $Fe_{75.5}Si_{13.5}B_9Cu_2$ alloy, " *J. Alloys and Comp*. vol. 475, no. 1-2, pp. 706-711, May. 2009.

[16] L. Kraus, O. Zivotsky, L. Postava, P. Svec, and D. Janiekovie, "Exchange Bias in Surface-Crystalline Fe-Nb-B Ribbons,"*IEEE Trans Magne.*, vol. 44, no. 11, pp. 3875-3878, Nov. 2008.

[17] M. S. Leu and T. S. Chin, "Quantitative crystallization fraction and nano-grain size distribution studies of a FeCuNbSiB amorphous alloy," *J. MRS Symp. Proc.*, pp. 557, 1999.

[18] W. M. Wang, Y. C. Niu, F. Wang, et. al., "Electrical resistivity evolution in the annealed amorphous $Fe_{78}Si_9B_{13}$ ribbons," *J. Non-Cry. Sol.*, vol. 354, no. 30, pp. 3612-3616, Jul. 2008.